



# The structure elucidation of the isomeric mixture of 3-[L-threo-2,3,4-tri-hydroxy-1-(phenyl-hydrazono)butyl]quinoxalin-2(1H)-one in dimethyl sulfoxide solution revisited: experimental and theoretical study

Mohamed A. El-Atawy<sup>1,2</sup> · Abdelrahman H. Hegazi<sup>3,2</sup> · Mohamed Al Khalaf<sup>3</sup> · Adel Amer<sup>3,2</sup>

Received: 6 September 2019 / Accepted: 24 October 2019 / Published online: 16 January 2020  
© Springer Science+Business Media, LLC, part of Springer Nature 2020

## Abstract

Based on the analyses of 1D and 2D NMR spectra techniques, such as H–H COSY, HSQC, and HMBC of 3-[L-threo-2,3,4-trihydroxy-1-(phenylhydrazono)butyl]-quinoxalin-2(1H)-one in dimethyl sulfoxide solution, it was concluded that this compound exists as a mixture of two isomeric Z- and E- forms I and II rather than the hydrazine imine and diazeny enamine V tautomers reported earlier. The NMR signals assignment was supported using density functional theory.

**Keywords** NMR · Quinoxaline · Hydrazone · Isomerism · DFT calculations

The hydrazone function containing molecules constitutes an important class of organic compounds. Its ubiquity and versatility can be attributed to its ease of synthesis [1–4] and most importantly unique structural properties, which enable its existence in different isomeric forms [5–9]. Isomerism involving this function group has been extensively investigated in the recent years [10–13]. Add to that, literature survey showed that hydrazones possess a wide variety of biological activities [14–18] besides their utilization as molecular switches, metallo-assemblies, and sensors [19–21] in which such isomeric forms play an imperative role.

We have reported on the structure of the multi component reaction of L-ascorbic acid **1**, o-phenylenediamine **2**, and phenylhydrazine **3** as 3-[L-threo-2,3,4-trihydroxy-1-(phenylhydrazono)butyl]quinoxalin-2(1H)-one or [3-((2S,3S)-2,3,4-trihydroxy-1-(2-phenylhydrazono)butyl)-quinoxalin-2(1H)-one] **4** rather than the cyclic structure **5** (Scheme 1) [22, 23].

The structure **4** gave the triacetoxy analogue **6**, which was secured by X-ray analysis [24]. Several reports were published concerning the syntheses of its analogues and showed their existence in two tautomeric forms with no definitive assignments given [25–29]. In 1990, we preferred the assignment of the two forms as hydrazone imine **I** and diazeny enamine **V** [24] as given for similar compounds [30] without perusing any evidence. Even though several reports were in support of such tautomerism for similar compounds, [5, 7] we have decided to re-investigate the isomerization of **4** in dimethyl sulfoxide solution using extensive 1D and 2D NMR techniques as well as density functional theory approach. The results are described and discussed.

**Electronic supplementary material** The online version of this article (<https://doi.org/10.1007/s11224-019-01445-3>) contains supplementary material, which is available to authorized users.

✉ Mohamed A. El-Atawy  
mohamed.elatawi@alexu.edu.eg

✉ Adel Amer  
aaamer@taibahu.edu.sa; adel.amer@alex-sci.edu.eg

<sup>1</sup> Chemistry Department, Faculty of Science, Taibah University, Yanbu 46423, Saudi Arabia

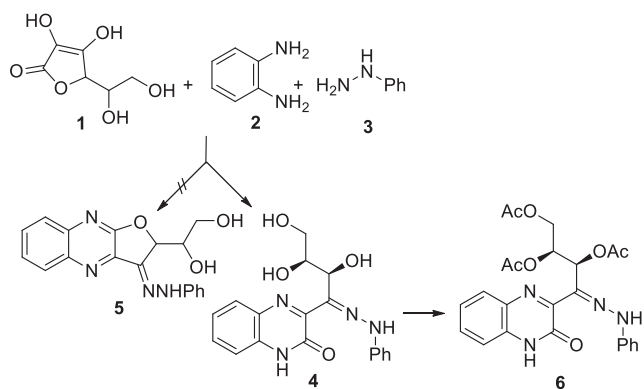
<sup>2</sup> Chemistry Department, Faculty of Science, Alexandria University, P.O. Box 426, Alexandria 21321, Egypt

<sup>3</sup> Chemistry Department, Faculty of Science, Taibah University, P.O. Box 30002, Al-Munawarah, Al-Madinah, Saudi Arabia

## Experimental

### Synthesis

<sup>1</sup>H-NMR and <sup>13</sup>C-NMR were recorded on Bruker 400 MHz spectrometers at ambient temperature. Chemical shifts ( $\delta$ ) are



**Scheme 1** Synthesis of hydrazone 4

quoted in parts per million (ppm) and are referenced to the residual solvent peak: DMSO-d<sub>6</sub>,  $\delta = 2.50$  ppm (1H),  $\delta = 39.52$  ppm (13C). In DEPT experiment (135°), the employed parameters were the following: time domain 65536; FID resolution 0.366798 Hz; acquisition mode 1.3631988 s; dwell time 20.800  $\mu$ s; pre-scan delay 6.00  $\mu$ s. The parameters in the COSYGPMFQF: time domain 2048; spectral width 5376.344 Hz; FID resolution 2.625168 Hz; acquisition time 0.1905140 s; receiver gain 2050; dwell time 93.000  $\mu$ s; prescan delay 6.00  $\mu$ s. The parameters in the COSYQF45: time domain 1024; spectral width 2762.431 Hz. The HSQCETGPSI2 parameters were the following: time domain 1024; spectral width 5376.344 Hz; FID resolution 5.250336 Hz; acquisition time 0.0952820 s; receiver gain 2050; dwell time 93.000  $\mu$ s; prescan delay 6.00  $\mu$ s. The

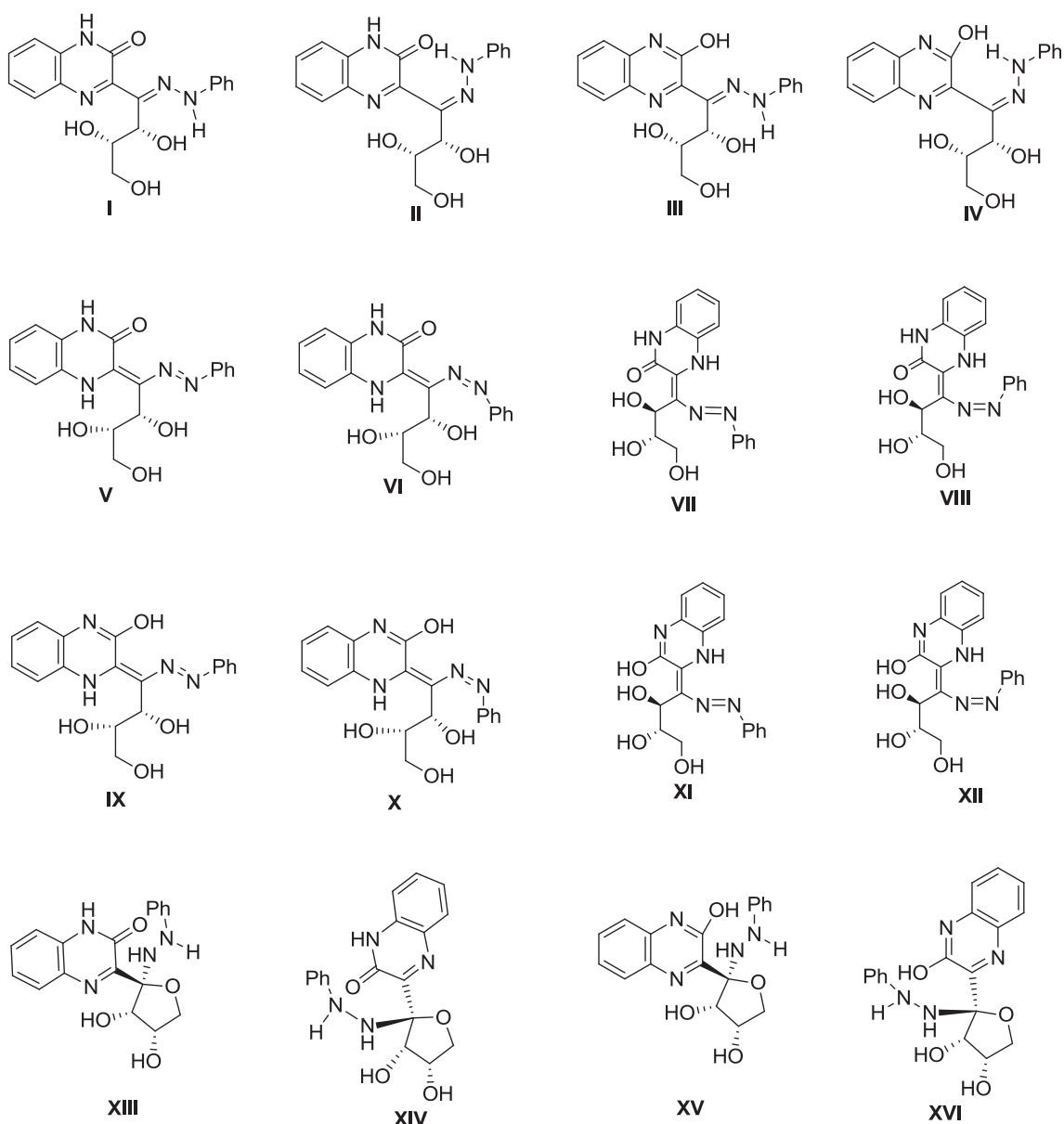


**Fig. 1** Illustration for the sixteen possible isomeric/tautomeric forms of 4

HMBC spectrum was determined with a pulse sequence GPNDQF: spectral width F2 (1H) 5376.344 and F1 (13C) 22321.429 Hz. Infrared spectra were recorded on Shimadzu FT-IR 8000S as KBr pellets, the absorption bands ( $\nu_{\max}$ )  $\text{cm}^{-1}$  (Fig. S1). Mass spectra were recorded on Bruker MALDI microflex mass spectrometer (Fig. S2).

Compound **4** was prepared as described earlier [22, 23]. The TLC, IR, and mass spectra were in agreement with authentic sample prepared earlier [24].

## Computational details

All calculations were performed using the GAUSSIAN 09 W [31]. Initially a conformational search for obtaining the most stable conformer was done using the semi-empirical PM3 method; the most stable conformer was subjected to full geometrical optimizations using DFT and Becke's three-parameter hybrid exchange functional in combination with the gradient-corrected correlation functional of Lee, Yang, and Parr B3LYP/cc-pvtz method [32–34]. For all optimizations, the vibrational frequencies were checked for imaginary frequencies to ensure all final geometries corresponded to a true minimum on the electronic potential energy surface.  $^1\text{H}$ -NMR and  $^{13}\text{C}$ -NMR shieldings of the previously optimized compounds have been calculated using gauge-including atomic orbital GIAO/B3LYP [35–37] density functional method with cc-pvtz basis set. To evaluate the relative chemical shifts, the tetramethylsilane (TMS) was optimized and then its shielding constants were calculated at the same level of theory. The calculated isotropic shieldings for TMS are 31.74 for  $^1\text{H}$  and 185.02 for  $^{13}\text{C}$  at the DFT-B3LYP level of theory, using the basis set cc-pvtz. The inclusion of solvent (dimethyl sulfoxide) in both structures optimization and NMR calculations was done via the inclusion of the polarisable continuum model (PCM) [38].

## Results and discussion

Theoretically sixteen isomeric/tautomeric structures hydrazone-imine-amide (Z and E), hydrazone-imine-iminol (Z and E), diazenyl enamine-amide, diazenyl enamine-iminol, and  $\alpha$ - and  $\beta$ -ring-chain forms I–XVI can be written for compound **4** (Fig. 1).

The NMR studies of **4** have not been reported in detailed before. In the present investigation, the  $^1\text{H}$ -NMR spectrum in dimethyl sulfoxide- $d_6$  ( $\text{DMSO-}d_6$ ) of **4** was obtained and shown in supplementary data (Fig. S3) as a mixture of two isomeric forms in 2:1 ratio (A and B). The structure and atom labeling of **4** is illustrated in Fig. 2.

### $^1\text{H}$ -NMR

The signals of the exchangeable protons (OHs and NHs) (Table 1) appeared at  $\delta$  4.43, 4.70, 5.12, 6.00, 10.26, 10.68,

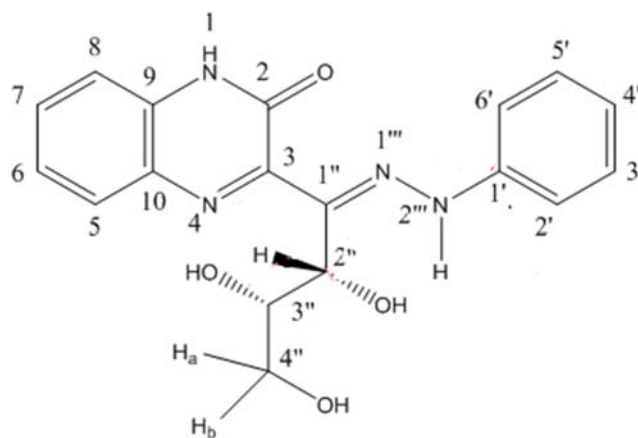


Fig. 2 Structure **4** with atom labeling scheme

and 12.54 ppm as broad singlets of 1.32 H, 1.00 H, 0.33 H, 0.33 H, 0.66 H, 0.33 H, and 1 H intensities, respectively. While the sugar moiety appeared as two multiplets at  $\delta$  3.43, 3.55, broad quartets at  $\delta$  3.79, 4.01 and doublet at  $\delta$  4.77 and 5.27 ppm (see Table 2). The phenyl group protons showed collapsed two triplet of triplets at  $\delta$  6.77 and 6.81, two doublet of doublets at  $\delta$  7.09, 7.23, two triplets at  $\delta$  7.19, 7.13, two multiplets at  $\delta$  7.35, 7.29, two doublet of doublets at  $\delta$  7.37, 7.32, triplet of doublets at  $\delta$  7.50, triplet of doublets at  $\delta$  7.59, doublet of doublets at  $\delta$  7.71, and doublet of doublets at  $\delta$  7.85 ppm (see Table 2). Moreover, assignments based on  $^1\text{H}$ - $^{13}\text{C}$  HSQC experiment for hydrogenated aromatic carbons are shown in Table 3 & for assignments see Fig. S3.

These assignments were supported by the two-dimensional  $^1\text{H}$ - $^1\text{H}$  COSYGPMFQF NMR (gradient-selected multiple-quantum-filtered COSY, Bruker pulse program). The COSY spectrum of **4** (Fig. S4) confirms the correlation assignments of H-4''s at  $\delta$  3.43, 3.55 (A and B) and H-3''s (A and B) at  $\delta$  3.79, 4.01. H-3''s show correlation with H-4'' and H-2''s of A and B at  $\delta$  4.77 and 5.27 ppm. Based on the correlation with protons of H-4'', H-3'', and H-2'' of A and B, one can assign the exchangeable Hs at  $\delta$  4.43 ppm for OHs on (C-2'' A and

**Table 1** Experimental chemical shift and assignment of the exchangeable protons of compound **4**

$\delta$ (ppm)	Intensity	Assignment
4.43	1.32 = 2(0.66) + 0(0.33)	2OH (A)
4.70	1.00 = 1(0.66) + 1(0.33)	OH (A) + OH (B)
5.12	0.33 = 0(0.66) + 1(0.33)	OH (B)
6.00	0.33 = 0(0.66) + 1(0.33)	OH (B)
10.26	0.66 = 1(0.66) + 0(0.33)	NH (A)
10.68	0.33 = 0(0.66) + 1(0.33)	NH (B)
12.54	1.00 = 1(0.66) + 1(0.33)	NH (A) + NH (B)

C-3" A), 4.70 ppm for OHs on (C-4" A and C-2" B), 5.12 ppm for OH on C-3" B, and 6.00 ppm for OH on C-4" B (Fig. S5).

In order to give more detailed explanation for the assignment of the exchangeable protons, the values of the peaks intensity have been divided according to the ratio 2:1 of the isomers A and B, respectively (Table 1). In addition, as indicated from the calculated chemical shift, that OHs are more shielded than NHs have also been considered. Accordingly, the peak at  $\delta$  4.43 ppm represents two hydroxyl groups of isomer A. While peak at  $\delta$  4.70 represents an overlapped peak for one hydroxyl group of each isomer. The other two hydroxyl group of minor isomers (B) appeared at  $\delta$  5.12 and 6.00 ppm, while its NHs appeared highly deshielded at 10.68 and 12.54.

Although the spectrum was clear for the aliphatic region, it showed a complicated pattern in the aromatic region. The  $^1\text{H}$ - $^1\text{H}$  COSYGP45 was then used instead (Fig. S6) and it was possible to assign the phenyl and quinoxaliny protons (Table 2). The expected splitting patterns of H-5 and H-8 as well as H-6 and H-7 should be the same. From the computational data, H-5 is the most deshielded one which appeared at  $\delta$  7.85 and 7.71 ppm for A and B isomers, respectively. As COSY indicates the correlation with coupled protons, it was concluded that the protons located at  $\delta$  (7.35, 7.29), (7.59, 7.50), and (7.37, 7.32) are correlated to each other and they were assigned for (H-6 A & B), (H-7 A & B), and (H-8 A & B), respectively. (Fig. S6).

### $^{13}\text{C}$ -NMR

The spectrum showed twenty-nine signals for both isomeric forms A & B (Fig. S7). From the DEPT 135 experiment (Fig.

**Table 2** Experimental and calculated  $^1\text{H}$ -NMR chemical shifts for compound 4 as a mixture of I and II

Assignment	Z-isomer		E-isomer	
	Exp. <sup>2</sup>	Calc. <sup>b</sup>	Exp. <sup>2</sup>	Calc. <sup>b</sup>
H <sub>a</sub> ,4", H <sub>b</sub> ,4"	3.43	3.82, 3.92	3.55	3.77, 3.99
H-3"	3.79	5.28	4.01	4.95
H-2"	4.77	5.11	5.27	4.43
H-4'	6.77	7.29	6.81	7.01
H-2' & H-6'	7.09	7.18, 7.45	7.23	6.81, 7.85
H-3' & H-5'	7.19	7.66, 7.45	7.13	7.35, 7.45
H-7	7.59	7.85	7.50	7.81
H-8	7.37	7.40	7.32	7.35
H-6	7.35	7.66	7.29	7.62
H-5	7.85	8.09	7.71	7.97
MAE <sup>c</sup> (ppm)	0.41		0.12	

<sup>a</sup> Exp. is the experimental chemical shift in dimethyl sulfoxide

<sup>b</sup> Calc. is the calculated chemical shift

<sup>c</sup> MAE is the mean absolute error

**Table 3** Aromatic CH carbon (in ppm) assignment from  $^1\text{H}$ - $^{13}\text{C}$  HSQC

Assignment	A	B
H-5/C-5	7.85/128.78	7.71/128.26
H-6/C-6	7.35/123.29	7.29/123.11
H-7/C-7	7.59/130.72	7.50/129.80
H-8/C-8	7.37/115.40	7.32/114.96
H-2', 6'/C-2', 6'	7.09/112.80	7.23/112.56
H-3', 5'/C-3', 5'	7.19/128.99	7.13/128.88
H-4'/C-4'	6.77/119.30	6.81/119.80

S8), the CH<sub>2</sub>, CH, and quaternary carbon signals were observed and overlapping of signals was confirmed.

### $^1\text{H}$ - $^{13}\text{C}$ HSQC

In DMSO-d<sub>6</sub>, the signals owing to C-4", C-3", and C-2" atoms of 4 were observed in the HSQC NMR spectrum at the  $\delta$  62.50 (A & B), 73.19 (A), 73.09 (B), and 72.76 (A), 70.62 (B), respectively (Fig. S9). The CH aromatic carbons were assigned based on their correlation with corresponding Hs (Fig. S10) and summarized in Table 3.

### $^1\text{H}$ - $^{13}\text{C}$ HMBC

The long-range HMBC (Fig. S11) cross peaks of 4 in DMSO-d<sub>6</sub> showed correlation between hydrazono NH 10.26 & 10.68 and C-1"  $\delta$  145.09 (A) and 144.63 (B), respectively, in addition to a clear correlation between the NH at  $\delta$  10.26 and C-2', C-6' at  $\delta$  112.80 (Fig. 3). These findings ruled out structures V–XII which lack the hydrazono proton.

Moreover, existence of correlation between H-2" 4.77 & 5.27 and C-1"  $\delta$  140.05 (A) and 140.83(B), respectively, secured the assignment of the C-1" resonance. Furthermore, the experimental chemical shift of C-1" ( $\delta$  140.05 (A) and 140.83(B)) is in accordance and good agreement with the calculated shift for C-1" ( $\approx$

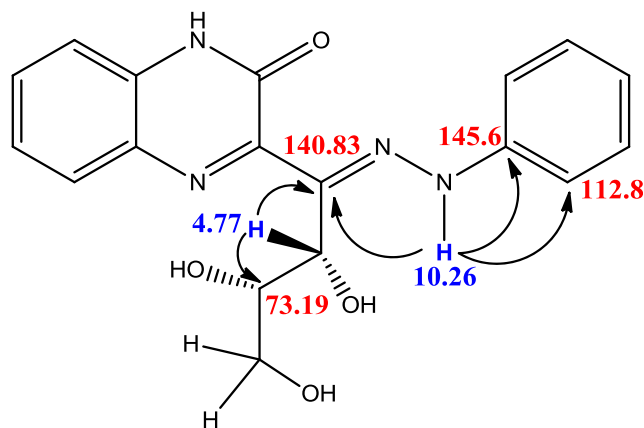


**Fig. 3** Structure 4 with carbon-hydrogen atoms correlation

**Table 4** Experimental and calculated  $^{13}\text{C}$ -NMR chemical shifts for compound 4 as a mixture of I and II

Assignment	Z-isomer		E-isomer	
	Exp. <sup>a</sup>	Calc. <sup>b</sup>	Exp. <sup>a</sup>	Calc. <sup>b</sup>
C-4''	62.50	72.03	62.50	58.90
C-2''	72.76	74.16	70.62	76.66
C-3''	73.19	82.16	73.09	67.97
C-2' & C-6'	112.80	118.96, 118.96	112.56	100.52, 103.13
C-8	115.40	119.70	114.96	105.13
C-4'	1119.30	127.09	119.80	110.31
C-7	130.72	137.68	129.80	122.94
C-5	128.78	135.80	128.26	120.74
C-3' & C-5'	128.99	135.70, 135.23	128.88	119.11, 119.66
C-6	123.29	129.40	123.11	114.96
C-9	131.85	139.20	131.42	121.57
C-10	132.23	139.20	132.23	123.71
C-1''	140.09	143.15	140.83	133.24
C-1'	145.09	150.70	144.63	134.71
C-2	154.22	160.03	154.24	142.70
C-3	153.70	160.20	153.70	143.39
MAE <sup>a</sup> (ppm)	6.80		7.19	

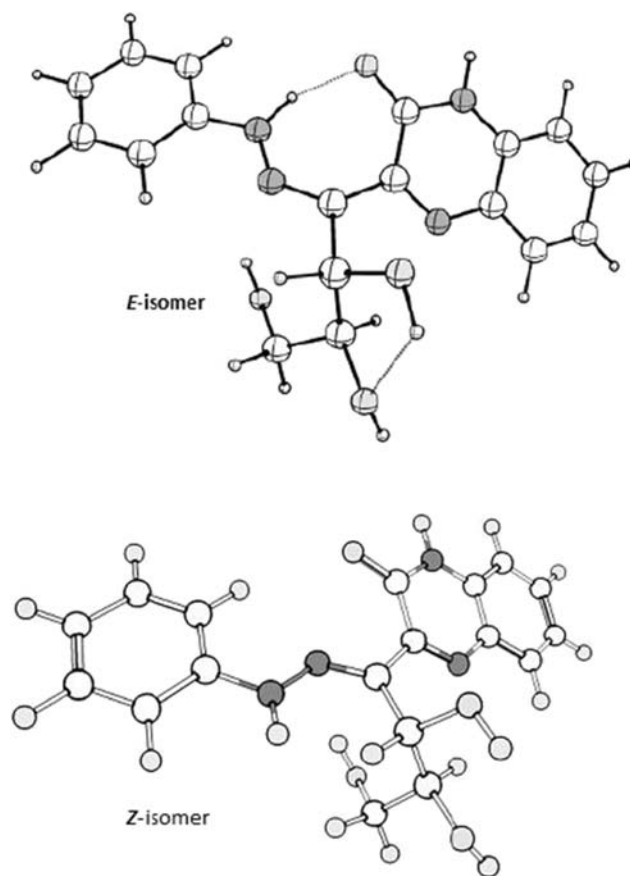
<sup>a</sup> Exp. is the experimental chemical shift in dimethyl sulfoxide

<sup>b</sup> Calc. is the calculated chemical shift

<sup>c</sup> MAE is the mean absolute error

143 ppm) of structures I–IV and quite far from the calculated shift (~ 100 ppm) for the  $\text{sp}^3$  carbon arising from cyclization of the sugar moiety in cyclic structures XIII–XVI. Accordingly, structures XIII–XVI were ruled out. Also, the 2D spectra showed the presence of correlation between the H-5  $\delta$  7.85 and 7.71 for both isomers and the carbon at  $\delta$  132.23 confirming that this resonance belongs to C-10. On the other hand, the correlation between H-8  $\delta$  7.37 and 7.32 and  $\delta$  131.85 and 131.42, respectively, lead to assigning this resonance to C-9. This leaves the remaining  $\delta$  153.70, 154.22, and 154.24 for C-3 and C-2 which their assignments were secured by the theoretical calculation (Table 4).

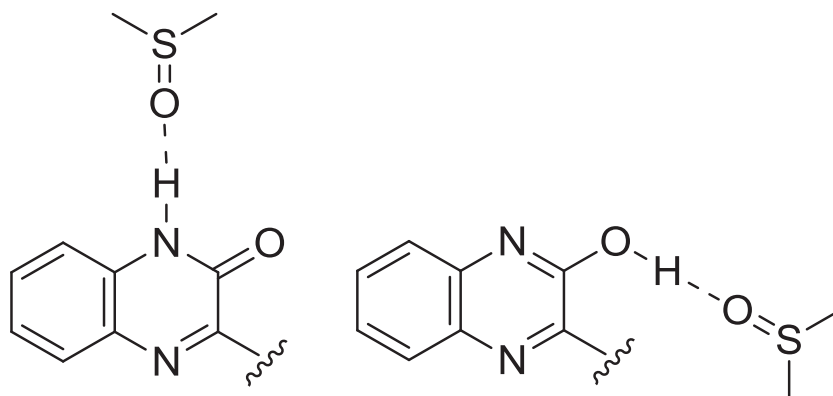
The stability of the quinoxalin-2(1*H*)-one structure (I and II) over the 2-hydroxyquinoxaline (III and IV) in dimethyl



**Fig. 5** The optimized structures of E- and Z-isomers of compound 4

sulfoxide solution could be explained by the complexation of 4 with dimethyl sulfoxide as a solvent via intermolecular hydrogen bonding that prefer N-H—O than O-H—O due to steric effect (Fig. 4). Moreover, dimethyl sulfoxide was reported to preferentially stabilize the more polar structures [39] which is the case in I and II over structures III and IV as indicated from their dipole moments. The complexation to the solvent was detected from  $^{13}\text{C}$ -NMR which showed two sets of resonances of dimethyl sulfoxide corresponding to complex structures with A and B (Fig. S12). Thus, structures III and IV are ruled out.

**Fig. 4** Possible representations of 4-dimethyl sulfoxide complex structures showing the intermolecular hydrogen bonding



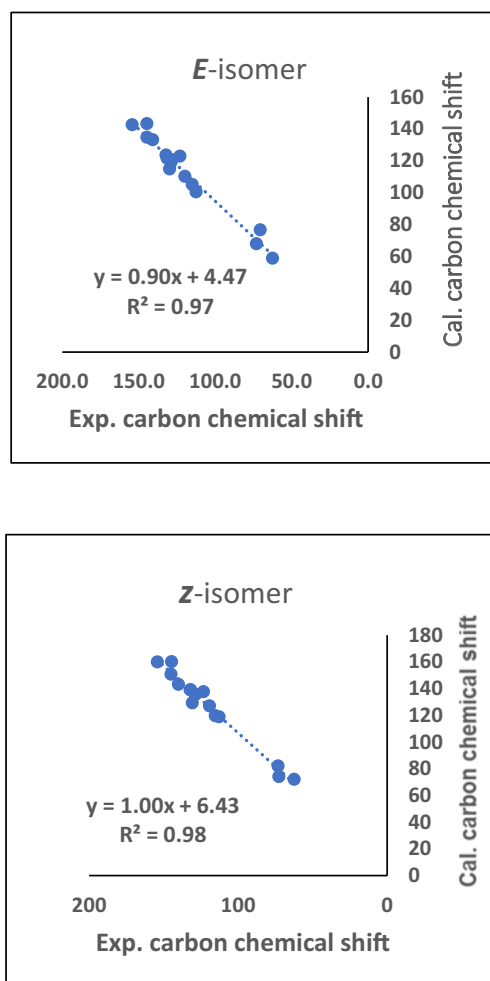


**Fig. 6** Plot of  $^{13}\text{C}$  exp. chemical shift vs calc. chemical shifts for compound **4**

### Molecular structure and optimized geometry

Optimized geometries of the two isomers **I** and **II** of compound **4** are shown in Fig. 5. The atomic labeling of the two isomers is shown in Figs. S13 and S14 in the supplementary data. The optimized geometrical parameters (bond length, angles, and dihedral angles) are listed in Table S1 which reveals that the geometry of E-isomer **II** enables it to form two intramolecular

**Table 5** DFT-calculated  $^1\text{H}$ NMR chemical shifts (ppm) for exchangeable protons of compound **4**

		Z-isomer	E-isomer
OH (C-2'')	(H38)	3.00	3.50
OH (C-3'')	(H37)	1.44	1.33
OH (C-4'')	(H36)	0.45	135
NH (N1)	(H27)	7.44	7.90
NH (N2''')	(H39)	7.89	11.00

Symbols between brackets represent the atom labeling in theoretical calculation

hydrogen bonds. The first one is between the last two hydroxyl groups of the sugar moiety (O..H-O with bond distance of 2.061 Å). The second one is between the oxygen of the carbonyl of the quinoxaline ring and the hydrogen of NH of the hydrazone moiety (O...H-N with distance of 1.850 Å). This was obviously noticed in the bond length of the hydrazone N-H where E-isomer **II** has relatively longer N-H (1.028 Å) than in Z-isomer **I** (1.016 Å). Another observation is that hydrogen bonded NH of E-isomer **II** vibrates at lower wave number (3293  $\text{cm}^{-1}$ ) relative to that of the Z-isomer (3512  $\text{cm}^{-1}$ ). This should be clear because hydrogen bond lengthens and weakens the N-H bond making it vibrates or stretches at lower energy.

### Calculated NMR spectra

Experimental and DFT-calculated chemical shifts (with respect to TMS) for all carbons and non-exchangeable protons of the Z- and E- isomers (**I** and **II**) of compound **4** are listed in Tables 2 and 4. The mean absolute error (MAE) is used to measure how close the calculated and experimental chemical shifts. Since the DFT-calculated chemical shifts for exchangeable protons is not reliable because it depends very highly on the dynamics, solvation, concentration, temperature, and etc. of the sample, it is not included in MAE calculations. MAEs were found to be 0.12 and 0.41 ppm as a result of comparison for experimental and calculated  $^1\text{H}$ -chemical shift of E- and Z-isomers, respectively, indicating quite similarity for the practical and predicted  $^1\text{H}$ -NMR chemical shifts. On the other hand, MAEs for carbon chemical shifts were found to be greater than 2 ppm for both isomers. This obviously shows the larger deviation of carbon chemical shifts from the experimental data than those of proton chemical shifts. To ensure that B3LYP findings for carbon chemical shifts are still in good agreement with the experimental data, their relationship was drawn in Fig. 6. It was found that there is an excellent linear relationship between the experimental carbon chemical shift and the theoretical shift with a linear correlation coefficient of  $R^2 = 0.98$  and  $0.97$ . This reveals slightly good fitting of the data.

DFT-calculated  $^1\text{H}$ -NMR chemical shifts for exchangeable protons are listed in Table 5. The calculations showed that the hydrogen of hydrazone NH of the E-isomer (appeared at 11.00 ppm) is more deshielded relative to that in the Z-isomer (appeared at 7.89 ppm). This could be explained on the basis that E-isomer is characterized by the N-H...O hydrogen bond. This HB makes the hydrogen located between two electronegative elements, namely, nitrogen and oxygen which makes hydrogen resonates at relatively high chemical shift causing the relative deshielding. While the Z-isomer lacks this effect. Furthermore, hydrogen atom of the hydroxyl group bonded to (C-2'') in E-isomer appeared at 3.50 ppm which is obviously more deshielded than that of the Z-isomer (3.00 ppm) due to the hydrogen bond formation in the former isomer. It is also noticed that OHs are more shielded than NHs for the two isomers (Table 5).

## Conclusion

The 1D and 2D NMR spectral data analysis confirmed the existence of compound **4** as an isomeric mixture of *Z* and *E* forms **I** and **II** rather than the hydrazone imine and diazeny enamine tautomers, and complete assignment for carbon and hydrogen atom signals is reported. Accordingly, the previous reported work should be corrected. It is worth noting that our present finding is in accordance with recently published work for similar system [40].

**Funding information** This work is supported by the Deanship of Scientific Research, Taibah University, SA (#7101).

## Compliance with ethical standards

**Conflict of interest** The authors declare that they have no conflict of interest.

## References

- Hernández-Vázquez E, Salgado-Barrera S, Ramírez-Espinosa JJ, Estrada-Soto S, Hernández-Luis F (2016) Synthesis and molecular docking of *N'*-arylidene-5-(4-chlorophenyl)-1-(3, 4-dichlorophenyl)-4-methyl-1H-pyrazole-3-carbohydrazides as novel hypoglycemic and antioxidant dual agents. *Bioorg Med Chem* 24: 2298–2306
- Le Goff G, Ouazzani J (2014) Natural hydrazine-containing compounds: biosynthesis, isolation, biological activities and synthesis. *Bioorg Med Chem* 22:6529–6544
- Amim RS, Firmino GS, Rego AC, Nery AL, Da-Silva SA, de Souza MV, Pessoa C, Resende JA, Figueroa-Villar JD, Lessa JA (2016) Cytotoxicity and leishmanicidal activity of isoniazid-derived hydrazones and 2-pyrazineformamide thiosemicarbazones. *J Braz Chem Soc* 27:769–777
- Chavan AS, Kharat AS, Bhosle MR, Mane RA (2018) Baker's yeast catalyzed one-pot synthesis of bioactive 2-[benzylidene (or pyrazol-4-ylmethylene) hydrazone]-1, 3-thiazolidin-4-one-5-yl-acetic acids. *Heterocycl Commun* 24:103–107
- Wojciechowska A, Jasiński M, Kaszyński P (2015) Tautomeric equilibrium in trifluoroacetaldehyde arylhydrazones. *Tetrahedron* 71:2349–2356
- Gordillo MA, Soto-Monsalve M, Carmona-Vargas CC, Gutiérrez G, D'vries RF, Lehn JM, Chaur MN (2017) Photochemical and electrochemical triggered bis (hydrazone) switch. *Chem Eur J* 23: 14872–14882
- Kumar SS, Biju S, Sadasivan V (2018) Synthesis, structure characterization and biological studies on a new aromatic hydrazone, 5-(2-(1, 5-dimethyl-3-oxo-2-phenyl-2, 3-dihydro-1H-pyrazol-4-yl) hydrazone)-2, 2-dimethyl-1, 3-dioxane-4, 6-dione, and its transition metal complexes. *J Mol Struct* 1156:201–209
- Mori A, Suzuki T, Sunatsuki Y, Kobayashi A, Kato M, Kojima M, Nakajima K (2014) Linkage and geometrical isomers of dichloridobis (triphenylphosphine) ruthenium (II) complexes with quinoline-2-carbaldehyde (Pyridine-2-carbonyl) hydrazone: their molecular structures and electrochemical and spectroscopic properties. *Eur J Inorg Chem*:186–197
- Šimůnek P, Padělková Z, Macháček V (2014) Solution and solid-state study of the structure of azo-coupling products from isomeric enamines possessing tert-butyl group: an unprecedented observation of pure hydrazo form in azo coupled *N*-alkyl  $\beta$ -enaminones. *J Mol Struct* 1075:187–195
- Galvão AM, Carvalho MFN, Ferreira AS (2016) Supramolecular arrangement in mono and bi-camphor acyl hydrazones: a structural study. *J Mol Struct* 1108:708–716
- Bagdatli E, Ocal N (2012) Synthesis, spectroscopic, and dyeing properties of new azo and bisazo dyes derived from 5-pyrazolones. *J Heterocyclic Chem* 49:1179–1186
- Fan Q, Wang Y, Yan H (2018) An NMR and DFT investigation on the interconversion of 9-substituted-*N*-6-hydrazone-8-azaadenine derivatives: proton migration or conformational isomerization? *Struct Chem* 29:871–879
- Kaya Y, Icel C, Yilmaz VT, Buyukgungor O (2015) Structural, spectroscopic and quantum chemical studies of acetyl hydrazone oxime and its palladium (II) and platinum (II) complexes. *J Mol Struct* 1095:51–60
- Kummari B, Ramesh P, Parsharamulu R, Allaka TR, Anantaramu H, Yogeewari P, Balasubramanian S, Guggilapu SD, Babu BN, Anireddy JS (2018) Design and synthesis of new etodolac-pyridazinones as potent anticancer agents using Pb (OAc) 4 to assist N-N bond formation. *ChemistrySelect* 3: 5050-5054.
- Coa JC, Castrillón W, Cardona W, Carda M, Ospina V, Muñoz JA, Vélez ID, Robledo SM (2015) Synthesis, leishmanicidal, trypanocidal and cytotoxic activity of quinoline-hydrazone hybrids. *Eur J Med Chem* 101:746–753
- Costa LB, de Oliveira Cardoso MV, de Oliveira Filho GB, de Moraes Gomes PAT, Espíndola JWP, de Jesus Silva TG, Torres PHM, Junior FPS, Martin J, de Figueiredo RCBQ (2016) Compound profiling and 3D-QSAR studies of hydrazone derivatives with activity against intracellular *Trypanosoma cruzi*. *Bioorg Med Chem* 24:1608–1618
- Souza LGS, Almeida MC, Lemos TL, Ribeiro PR, de Brito ES, Silva VL, Silva AM, Braz-Filho R, Costa JG, Rodrigues FF (2016) Synthesis, antibacterial and cytotoxic activities of new biflorin-based hydrazones and oximes. *Bioorg Med Chem Lett* 26:435–439
- Palanimuthu D, Wu Z, Jansson PJ, Braidy N, Bernhardt PV, Richardson DR, Kalinowski DS (2018) Novel chelators based on adamantane-derived semicarbazones and hydrazones that target multiple hallmarks of Alzheimer's disease. *Dalton Trans* 47: 7190–7205
- Gupta VK, Singh AK, Bhardwaj S, Bandi KR (2014) Biological active novel 2, 4-dinitro phenyl hydrazones as the colorimetric sensors for selective detection of acetate ion. *Sensors Actuators B Chem* 197:264–273
- Nakatsuka N, Bamaby SN, Fath KR, Banerjee IA (2012) Fabrication of collagen-elastin-bound peptide microtubes for mammalian cell attachment. *J Biomater Sci Polym Ed* 23: 1843-1862.
- Ganjali MR, Rezapour M, Rasoolipour S, Norouzi P, Adib M (2007) Application of pyridine-2-carbaldehyde-2-(4-methyl-1, 3-benzo thiazol-2-yl) hydrazone as a neutral ionophore in the construction of a novel Er (III) Sensor. *J Braz Chem Soc* 18:352–358
- El Ashry ESH, El Kholy IE, El Kilany Y (1978) Dehydrative ring-closure of 3-substituted 2-quinoxalinones to give fused and nonfused pyrazoloquinoxalines. *Carbohydr Res* 60:303–314
- Henseke G, Dittrich K (1959) Heterocyclische Verbindungen, VI Chinoxaline synthesen mit Dehydro-L-ascorbinsäure. *Chem Ber* 92:1550–1558
- Amer A, Massry AM, Awad L, Rashed N, El Ashry ESH, Ho D (1990) Structure of the reaction products from dehydroascorbic acid analogues, o-phenylenediamine, and arylhydrazines. X-Ray molecular structure of 3-[L-threo-2, 3, 4-triacetoxy-1-(phenylhydrazone) butyl] quinoxalin-2 (1 H)-one hemihydrate. *J Chem Soc Perkin Trans* 1:2513–2518
- El Ashry ESH, Rahman MMA, Nassr MA, Amer A (1978) Transformation of the hydrazones of 6-chloro-3-(l-threo-2, 3, 4-

- trihydroxy-1-oxobutyl)-2-quinoxalinone into other heterocyclic compounds. *Carbohydr Res* 67:403–414
26. El Ashry ESH, Rahman MMA, Rashed N, Amer A (1978) Reaction of dehydro-d-erythorbic acid and its aryl analogs with ortho-diamines. *Carbohydr Res* 67:423–432
  27. Amer A, Ho D (1992) Synthesis and structural elucidation of the acetylation reaction's product (s) of the 2 (1H)-quinoxalinones derived from L-ascorbic acid. X-ray molecular structure of 3-(N-acetyl-2-naphthylhydrazono)-2, 3-dihydro-2-acetoxifuro [2, 3-b] quinoxaline. *Zeitschrift für Naturforschung B* 47: 861-868.
  28. El Ashry ESH, Atta KF, Aboul-Ela S, Beldi R (2007) MAOS of quinoxalines, conjugated pyrazolylquinoxalines and fused pyrazoloquinoxalines from l-ascorbic and d-isoascorbic acid. *J Carbohydr Chem* 26: 1-16.
  29. Awad LF (2000) Isolation and identification of the intermediates during pyrazole formation of some carbohydrate hydrazone derivatives. *Carbohydr Res* 326:34–42
  30. Kurasawa Y, Muramatsu M, Yamazaki K, Tajima S, Okamoto Y, Takada A (1986) Tautomeric behavior of 3-( $\alpha$ -arylhydrazono) methyl-2-oxo-1, 2-dihydroquinoxalines between hydrazone imine and diazenyl enamine forms. *J Heterocyclic Chem* 23:1245–1248
  31. Frisch MJ, Trucks GW, Schlegel H.B, Scuseria G E, Robb MA, Cheeseman J R, Montgomery Jr JA, Vreven T, Kudin KN, Burant JC, Millam JM, Iyengar SS, Tomasi J, Barone V, Mennucci B, Cossi M, Scalmani G, Rega N, Petersson GA, Nakatsuji H, Hada M, Ehara M, Toyota K, Fukuda R, Hasegawa J, Ishida M, Nakajima T, Honda Y, Kitao O, Nakai H, Klene M, Li X, Knox JE, Hratchian HP, Cross JB, Bakken V, Adamo C, Jaramillo J, Gomperts R, Stratmann RE, Yazyev O, Austin AJ, Cammi R, Pomelli C, Ochterski JW, Ayala PY, Morokuma K, Voth GA, Salvador P, Dannenberg JJ, Zakrzewski VG, Dapprich S, Daniels AD, Strain MC, Farkas O, Malick DK, Rabuck AD, Raghavachari K, Foresman JB, Ortiz JV, Cui Q, Baboul AG, Clifford S, Cioslowski J, Stefanov BB, Liu G, Liashenko A, Piskorz P, Komaromi I, Martin RL, Fox DJ, Keith T, AlLaham MA, Peng CY, Nanayakkara A, Challacombe M, Gill PMW, Johnson B, Chen W, Wong MW, Gonzalez C, Pople JA (2009) Gaussian, Inc., Wallingford CT 121: 150-166.
  32. Becke AD (1993) Density-functional thermochemistry. III The role of exact exchange. *J Chem Phys* 98:5648–5652
  33. Lee C, Yang W, Parr RG (1988) Development of the Colle-Salvetti correlation-energy formula into a functional of the electron density. *Phys Rev B* 37:785–789
  34. Hariharan P, Pople JA (1972) The effect of d-functions on molecular orbital energies for hydrocarbons. *Chem Phys Lett* 16:217–219
  35. Ramos J.M, Faget G, Felcman J, Téllez CA (2008) Fourier transform infrared and Raman spectra, and AB initio calculations for cadmium (II)-cysteinate glycinate complex [Cd (Cys)(Gly)]. *Spectrochim. Acta Part A* 71: 1364-1370; Erratum to“Fourier transform infrared and Raman spectra, and AB initio calculations for cadmium (II)-cysteinate glycinate complex [Cd (Cys)(Gly)]”[*Spectrochim. Acta Part A* 71 (2008) 1364-1370], (2009) *Spectrochimica acta Part A: molecular spectroscopy* 72: 228-228.
  36. Parlak C, Alver Ö, Şenyel M (2008) Experimental and theoretical NMR study of 4-(3-cyclohexen-1-yl) pyridine. *Spectrochim Acta A Mol Biomol Spectrosc* 69:1252–1256
  37. Bagno A, Rastrelli F, Saielli G (2006) Toward the complete prediction of the 1H and 13C NMR spectra of complex organic molecules by DFT methods: application to natural substances. *Chem Eur J* 12: 5514–5525
  38. Scalmani G, Frisch MJ (2010) Continuous surface charge polarizable continuum models of solvation. I. General formalism. *J chem physics* 132: 114110.
  39. Gomez JA, Lage MR, Cameiro JWdM, Resende JA, Vargas MDT (2013) Tautomerism in quinoxalines derived from the 1,4-naphthoquinone nucleus: acid mediated synthesis, X-ray molecular structure of 5-chlorobenzo[f]quinoxalin-6-ol and density functional theory calculations. *J Braz Chem Soc* 24: 219-229.
  40. Lyčka A (2019) 15 N, 13C and 1H NMR study of tautomerism and *E/Z* isomerism in 3-[(*Z*)-(2-phenyl-hydrazinylidene)methyl]quinoxalin-2(1*H*)-one and 3-[(*E*)-(2-phenylhydrazinylidene)methyl]quinoxalin-2(1*H*)-one. *Dyes Pigments* 165:341–345

**Publisher's note** Springer Nature remains neutral with regard to jurisdictional claims in published maps and institutional affiliations.